Surface Texture Measurements of CMP Pads Using a Flow-Based Characterization Test

Ravi Palaparthi and Gregory P. Muldowney
Advanced Research Group
Rohm and Haas Electronic Materials CMP Technologies, Newark, DE 19713 ©2004

Prepared for Presentation at National AIChE Meeting, Austin, TX, November 8, 2004
Session T8003 – Electropolishing and Chemical Mechanical Planarization (CMP) Paper #93e

Unpublished

AIChE Shall Not Be Responsible for Statements or Opinions Contained in Papers or Printed in its Publications

Abstract

Surface texture of CMP polishing pads strongly affects the fluid mechanics of the polishing slurry and the state of pad-wafer contact. A flow-based texture characterization, using fluid pressure drop profiles measured across pad samples compressed by a flat instrumented plate, shows the extent of pad contact, the flow uniformity, and the relative contributions of viscous and inertial flow among the pad asperities. This characterization provides insights into the surface texture of different hard pad materials subjected to varying degrees of surface conditioning. Surface flow resistance, derived from the pressure profiles, correlates more closely with the removal rate and defect count observed in wafer polish tests than does purely physical texture measures such as average roughness. Results illustrate the essential role of pad compliance and slurry micro-mixing in CMP performance.

Keywords: CMP, polishing pad, surface texture, porous media, conditioning.

Introduction

In any CMP process, slurry conveyance to and under the wafer is highly dependent on both the pad surface texture and the groove network formed in the pad surface. While grooves may be rendered according to an exact geometry, surface texture is realized more indirectly through the inherent pad microstructure and by conditioning prior to and during polishing. Texture is also more difficult to measure and quantify as it is fundamentally a physical feature but manifests in polishing only through interaction with the wafer surface and the slurry flow field.

Surface conditioning is well known to impact CMP pad performance. The action of a conditioning disk is to cut or plow microscopic furrows into the pad material, creating a population of asperities (Figure 1). Much of the complexity of CMP lies in the interplay between contact mechanics at the asperity tips, which abrade off chemically softened wafer material, and slurry transport through the asperity layer, which supplies fresh reactants and abrasive particles and conveys away polish debris and heat.

The present work focuses on pad surface texture as a medium offering a resistance to slurry flow, and examines the response of this resistance to pad material, degree of conditioning, and applied downforce. Wafer polish data are analyzed to establish the texture properties that are most deterministic in removal rates and to gain insights about the critical mechanisms of CMP at the texture scale.

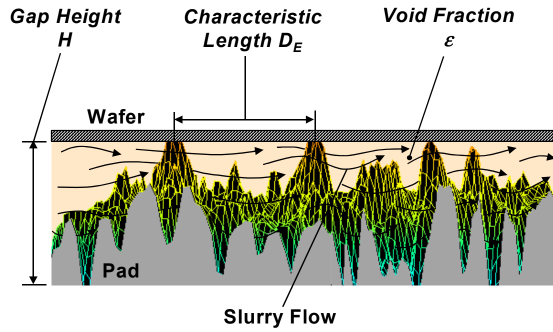

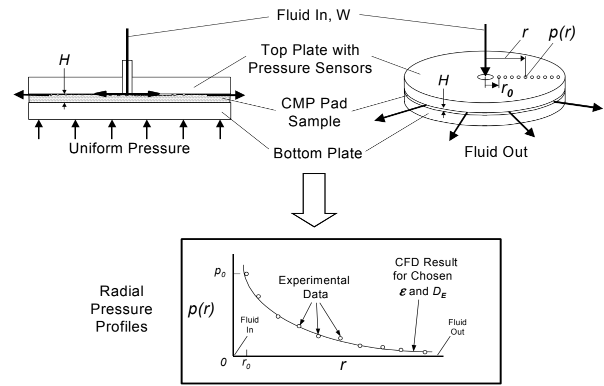

Figure 1: Surface Topography of CMP Pad

Figure 2: Flow-Based Pad Texture Measurement

Background

Prior to 2003, published models of wafer-scale slurry transport in CMP represented the pad-wafer gap using the Reynolds hydrodynamic equation[1,2,3], sometimes with enhancements to capture the effect of rough surfaces on the volume flow of slurry conveyed[4]. While adequate for predicting global velocity and temperature fields under the wafer for an *ungrooved* CMP pad, the lubrication approximation does not accurately capture the sharp disparities in transport fields that may prevail on grooved pads[5] nor the inertial flow effects that are possible within the texture of a pad.

If transport models of CMP have been oversimplified, it is partly because pad texture characterization has been limited to physical measurements with no clear connection to actual behavior during polishing. Stylus profilometry, optical and electron microscopy, and optical interferometry have all had utility for describing pad texture, but these techniques deliver composite geometric parameters such as average roughness (Ra) rather than descriptors of the pad-wafer and pad-slurry interactions.

In 2003, a porous-media flow approach was introduced[6] to characterize CMP pad surfaces (Figure 2). Instead of describing the texture topographically, the effective architecture of the asperity layer is deduced by forcing fluid over the pad surface while compressed between two flat plates and measuring the resulting pressure loss profiles. The pressure losses give a more realistic picture of the pad-slurry interaction under the wafer in a typical polish process, and lead to texture descriptors suitable for direct use in computational fluid dynamics (CFD) simulations.

Subsequent CFD studies using flow-based texture descriptors[7,8] have demonstrated that transport fields in the pad-wafer gap may depart significantly from those predicted by lubrication theory. For example, it has been shown that pad texture has at least as large an impact as wafer rotation speed on the steady-state temperature field under the wafer[9], and that interactions between texture and pad-wafer relative velocity determine how effectively fresh slurry replaces spent slurry[10].

Flow-based characterization of soft (Type II[11]) CMP pads has revealed that materials having vertical pores impart an inertial contribution to the pressure loss of fluid moving through the asperity layer[12], a key connection between pad microstructure and transport behavior. It is of interest to extend this understanding to hard (Type III[11]) pad texture in terms of slurry flow response to material type, degree of conditioning, and downforce to fully optimize CMP consumables for specific applications.

Experimental Apparatus and Scope

The flow-based texture characterization apparatus is detailed elsewhere[6] and consists of two 200-mm diameter flat plates between which a pad sample of the same size is mounted. A hydraulic lift applies a controlled pressure to raise the bottom plate and bring the pad into contact with the top plate. Fluid enters through a central inlet in the top plate, flows out radially through the compressed asperity layer of the sample, and exits at the perimeter. A polar grid of sensors on the top plate captures the pressure field $p(r,\theta)$ due to fluid flow over the pad surface. Sensors are accurate to 0.1 psi and are located in groups of ten (every 9.5 mm) along twelve radii 30 degrees apart. Such a distribution is obtained at several flow rates spanning the range of viscous and inertial fluid forces (μu and ρu^2) in commercial polishers. Pad samples are analyzed at multiple downforces from 0.5 to 8 psi, the range of industrial CMP practice.

Three comparative studies are conducted here. First, ungrooved samples of two different pad materials are conditioned for various times, using Kinik medium-aggressive discs with blocky or cubic octahedral diamonds, then tested for surface flow resistance to determine how the pad texture is modified. Second, grooved pads of one material type are prepared having different surface roughnesses to examine how roughness impacts surface flow resistance. Roughness is measured using a Wyko RollScope® optical profiler and a Hommelwerke LV-50 profilometer. Third, the pads of varying roughness are used to polish TEOS, copper, and TaN sheet wafers on a Mirra® tool using an experimental barrier slurry to investigate which surface descriptors best track CMP removal rates and defectivity. Removal rates are measured on a CDE ResMap 168 and scratch defect counts on an Orbot™ WF-720 tool.

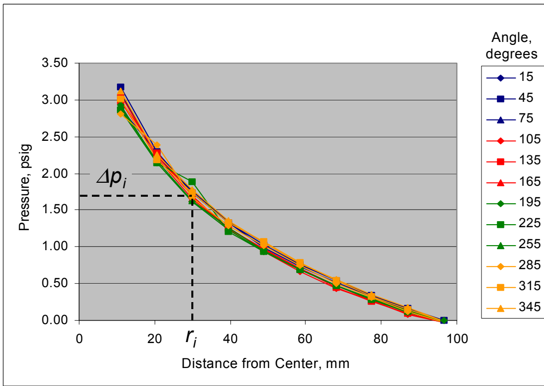

Figure 3: Pressure Profiles for Flow across Compressed CMP Pad Sample

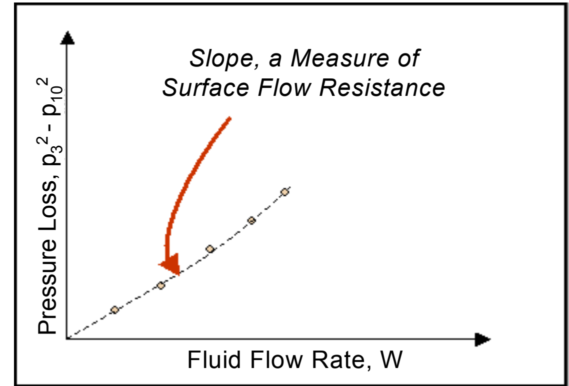

Figure 4: Determination of Surface Flow Resistance from Pressure Loss at Various Flow Rates

Data Analysis

Figure 3 shows radial pressure profiles obtained by flowing gas across the compressed surface of a typical hard CMP pad. For samples showing an axially symmetric pressure distribution, as in the earlier work[6], the pad-plate gap is modeled as a porous medium having a characteristic void fraction ε and length scale D_E. Noting in the present study that the fluid is compressible, the pressure drop p between two radial locations r_1 and r_2 under a mass flow rate W is described, based on the Ergun equation[13], as:

$$p(r_1)^2 - p(r_2)^2 = \left(\frac{\alpha RT\mu \cdot}{\pi M} \cdot \frac{(1-\varepsilon)^2}{HD_E{}^2\varepsilon^3}\right) \cdot W \ln\frac{r_2}{r_1} + \left(\frac{\beta RT}{2\pi^2 M} \cdot \frac{(1-\varepsilon)}{H^2 D_E \varepsilon^3}\right) \cdot W^2\left(\frac{1}{r_1} - \frac{1}{r_2}\right) \qquad (1)$$

where H is the effective fluid flow height between the pad surface and the top plate (typically equal to the asperity layer thickness), μ and M are the fluid viscosity and molecular weight, T is the temperature, R is the gas constant, and α and β are the viscous and inertial constants of the Ergun equation.

Plotting the difference of squared pressures between two fixed radii at various flow rates determines the pad surface flow resistance (Figure 4). Because the first two locations sometimes manifest entrance effects, the square difference is taken between the 3rd and 10th locations. Equation (1) is thus used as:

$$p(r_3)^2 - p(r_{10})^2 = AW + BW^2 \qquad (2)$$

where A and B are characteristic of the pad surface compressed under a given downforce. The terms AW and BW^2 represent the respective contributions of viscous and inertial flow in the pad-plate gap. Hence the percent inertial contribution is $100BW^2/(AW+BW^2)$, which may be positive or zero, and is compared across cases with respect to an average Reynolds number defined as $Re = W(r_{10}-r_3)/2\pi\mu \ln(r_{10}/r_3)$.

Results and Discussion

Effect of Hard Pad Surface Conditioning

Figure 5 compares results for hard pad types X and Y (X being softer than Y), unconditioned and after conditioning for 10 and 600 seconds, at various downforces. In both materials, surface flow resistance under a given downforce increases with conditioning time over 0 to 600 seconds. One way conditioning increases flow resistance is to render the asperities more finely divided such that the surface-to-volume ratio of the layer is greater, which decreases D_E in equation (1). Another probable mechanism is that conditioning renders the asperity layer more compliant to the top plate and creates a more uniformly obstructed flow domain having a smaller ε and imparting a higher pressure drop. The asperity layer may become more compliant by acquiring a narrower height distribution, for example by losing the tallest peaks of the original structure, leading to a larger population of peaks in contact or near-contact with the top plate. At any downforce and level of conditioning, fluid experiences higher pressure drop flowing over the surface of pad type X versus type Y. This indicates that using pad type X the pad-plate gap has more asperities obstructing the flow or that the asperity structure has a higher surface:volume, or both.

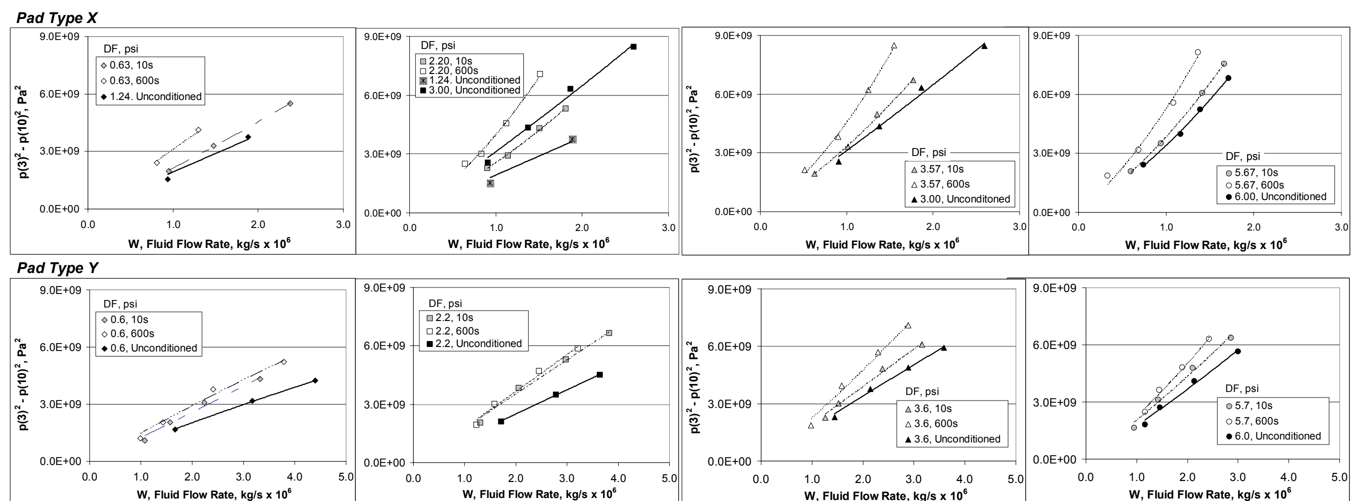

Figure 5: Comparison of Surface Flow Resistance of Hard Pad Types X (top) and Y (bottom) at Various Degrees of Surface Conditioning and Applied Downforce

Pad Type X

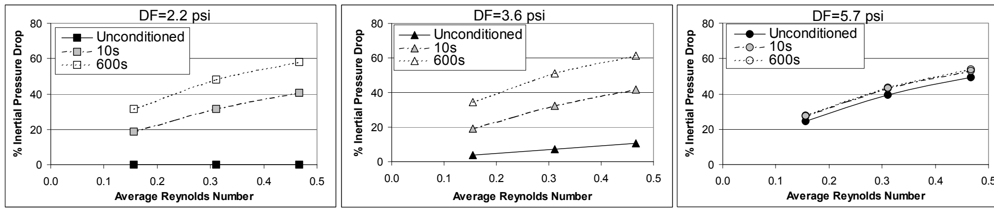

Pad Type Y

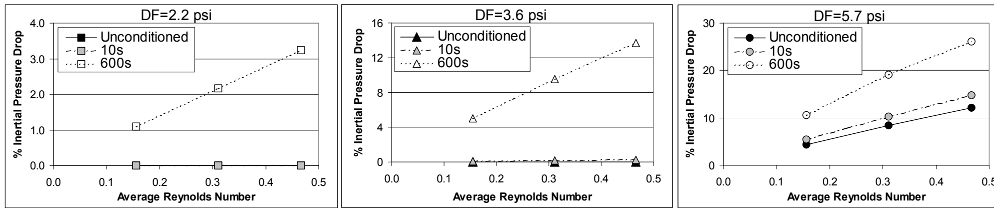

Figure 6: Comparison of Percent Inertial Pressure Drop of Hard Pad Types X (top) and Y (bottom) at Various Degrees of Surface Conditioning and Applied Downforce

Figure 6 shows the percent inertial loss for pad types X and Y. Under a given downforce, both materials induce a larger relative contribution of inertial flow as the pad is conditioned. On an unconditioned pad, long-wavelength thickness variations create an uneven pad-plate gap having many thin open spaces for flow, and viscous drag on the confining surfaces dominates the pressure drop. With greater conditioning, the pad surface becomes more uniformly populated with asperities of smaller length scales and the pad-plate gap more closely approaches a uniform porous medium. In the latter state, fluid dissipates more energy via frequent changes in direction and cross-section, inducing more inertial pressure drop. Higher inertial loss is thus tantamount to micro-mixing, and pad conditioning should favor good replacement of spent slurry with fresh slurry. Pad material dictates how rapidly inertial loss (read compliance) increases with conditioning: after ten seconds, pad type Y barely changes behavior while pad type X shows over half the inertial loss it will reach in ten minutes. Type X pads thus require less conditioning to induce a given level of slurry micro-mixing, allowing CMP pad break-in times to be significantly shorter.

Higher downforce also leads to greater inertial pressure drop within each pad type because the impact of long-wavelength variations is reduced and more uniform pad-plate contact is achieved. For pad type X, raising downforce from 2.2 to 5.7 psi increases the inertial loss contribution at a given Reynolds number significantly for the unconditioned pad but negligibly for the pad conditioned for 600 sec. (However the pressure drop itself increases at higher downforce as noted in Figure 5). This result reveals that the pad conditioned for 600 seconds is in full compliance with the plate even at lower downforces. By contrast, the same downforce increase produces a response in inertial contribution on all samples of pad type Y, indicating that even after conditioning for 600 seconds the surface has not reached its ultimate state of compliance. These findings illustrate the paramount importance of pad conditioning. Since downforce may vary point-to-point and over time in commercial CMP tools, the most uniform polish will result when pad-wafer compliance is independent of downforce.

Effect of Hard Pad Surface Roughness

Table I presents measured surface roughness pre- and post-polish for three samples of hard pad type Z. Roughness variations were achieved via slight changes in the manufacturing process. All the pads have standard concentric circular grooves and are tested for surface flow resistance *after* polishing.

Table I: Relative Surface Roughness (Ra/Ra_0) of Pad Samples

Pad ID	Relative Surface Roughness	
	As Manufactured*	Post-Polishing**
Low	1.0	1.0
Mid	1.9	1.4
High	2.3	1.3

* Measured with Hommelwerke LV-50
** Measured with Wyko RollScope

Figure 7 shows pressure drops for fluid flow in the pad-plate gap for the three pad roughness cases. At the lowest downforce (1.2 psi), fluid pressure drop and surface flow resistance (slope) are similar across all roughness levels. At higher downforce (3 psi), an ordering emerges whereby the resistance of the low-roughness pad is larger than that of the mid-roughness pad, which is in turn slightly larger than that of the high-roughness pad. At still higher downforces (5.8 and 8 psi), the low-roughness pad resistance becomes substantially larger than that of the mid-roughness pad, which maintains a small but constant margin over the high-roughness pad.

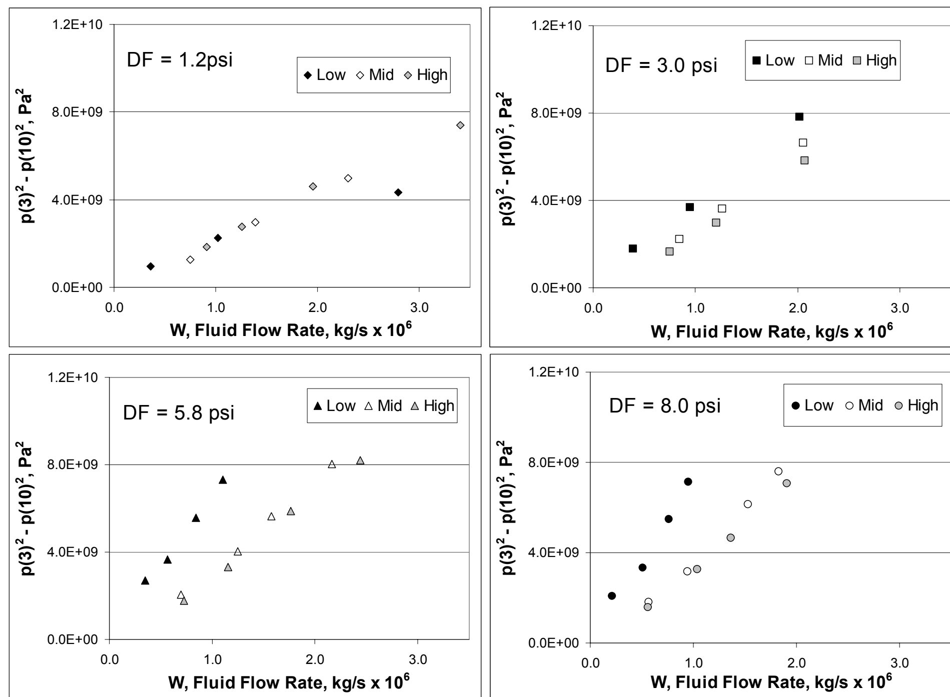

Figure 7: Surface Flow Resistance for Grooved Hard Pads of Low, Mid, and High Roughness at Various Applied Downforces

At fixed downforce, the decrease in surface flow resistance with increasing roughness is in agreement with earlier observations for soft pads[12] and reflects the larger void fraction that typically accompanies higher roughness. However for soft pads it was found that roughness was a strong influence at low downforces (1-2 psi) but a weaker factor at higher downforces (4-6 psi) where it was theorized that most surface voids were collapsed. This trend appears reversed for hard pads (Figure 7), the roughness effect being stronger at *higher* downforces. In fact the contrast illustrates two different states in the continuum of pad compliance. Due to its higher stiffness, the hard pad is less compliant to the top plate at lower downforces and the effect of surface roughness is dwarfed, while at higher downforces the compliance increases and roughness begins to manifest in the surface flow resistance. Under the same downforces,

a soft pad is already at or approaching full compliance. Deformation of surface voids theorized in soft pads probably occurs in hard pads as well, but only at much higher downforces not common in CMP. These results show that a broad spectrum of pad surface characteristics exist over the practical range of polish downforce, and that hard and soft pads will have entirely different responses within this range.

Hard Pad Surface Flow Resistance and Polishing Performance

Figure 8 shows copper, TEOS, and TaN removal rates obtained at 3 psi downforce using the same slurry chemistry with the pads of three roughness levels, plotted against the surface flow resistances calculated from the 3-psi data lines of Figure 7. Removal rates of all materials are highest with the low-roughness pad, lower with the mid-roughness pad, and slightly lower still with the high-roughness pad. While these rates do *not* correlate with the post-polish pad roughness values in Table I, they form a clear and linear response to surface flow resistance. As noted earlier, one source of higher surface flow resistance is a larger number of asperities in contact or near-contact with the confining surface—a state that also favors greater material removal under a fixed downforce. This finding corroborates earlier CFD simulations[9] that predict higher removal rate using finer pad textures offering greater resistance to slurry flow.

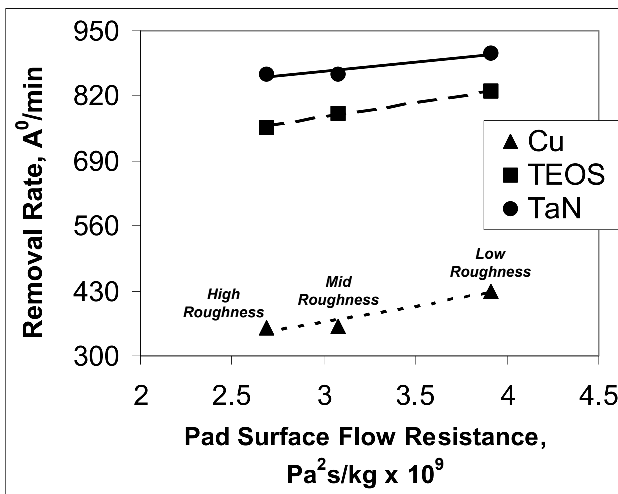

Figure 8: Removal Rates of Cu, TEOS, and TaN Using Pads of Variable Roughness

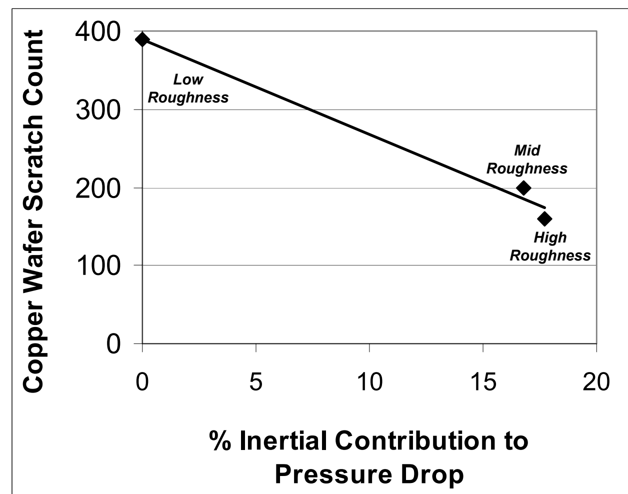

Figure 9: Scratch Defect Counts on Copper Wafers Using Pads of Variable Roughness

For copper polishing, low defectivity is often more critical than removal rate. Figure 9 shows copper wafer scratch counts from the polish tests plotted against the inertial contribution to pressure drop from the texture characterization tests (based on the 3-psi data of Figure 7 and a mass flow rate of 10^{-6} kg/s). Scratch count decreases strongly as the flow across the pad surface takes on a more inertial character. As noted above, higher inertial loss implies micro-mixing, more uniform exposure of the wafer to fresh slurry, and more effective removal of spent slurry. Polish debris and spent abrasive particles are thus less likely to form scratch defects when the pad surface induces flow patterns having a larger inertial influence. There are of course other mechanical aspects of polishing that contribute to defectivity and that vary among the three roughness levels. To date, however, no single pad mechanical property has been identified that quantitatively tracks both removal rate and defect count. Figure 9 implies that the slurry flow character imparted by the asperities, as much as the physical structure of the asperities, may be responsible for the pad-particle-wafer interactions that lead to defects. In this interpretation, defect reduction may be achieved through changes in the pad texture or the slurry constitution, or both.

Conclusions

The relationships presented in Figures 8 and 9 support the premise that transport phenomena at the scale of pad surface texture may determine polish performance, but are by no means a proof of causality. At the least, the foregoing results show that surface flow resistance serves as a better characterization of CMP pad texture than conventional measures such as average roughness. Surface flow resistance also provides a sound framework to interpret the effects of conditioning and downforce on the state of pad-wafer contact. This reflects the fact that the pressure drop of fluid flow in a porous medium reports the full three-dimensional nature of the structure under the applied downforce rather than a mere surface description.

Unsurprisingly, surface flow resistances for hard pads indicate a much lower degree of compliance than for soft pads. It follows that CMP using hard pads probably occurs on islands of good contact separated by oceans of poor contact, whereas soft pad contact is comparatively homogeneous. Higher defect counts associated with hard pads may arise not only from the intrinsic stiffness of the material, but also from the vanishing flow spaces at the boundaries of poor-contact regions that can trap and agglomerate particulate debris. In this regard, it is noteworthy that substantial differences in the extent of contact are observed even among hard pad variants. The trend in CMP to lower downforce polishing will produce different and potentially inverse responses in pad-wafer interaction between hard and soft materials. An opportunity clearly exists for hybrid pad formulations that capture the benefits of both extremes.

Acknowledgments

Polish results cited in this study were obtained by Todd Crkvenac and Scott Koons, who also assisted with data interpretation. The study benefited as well from contributions by Chris Juras, Jeff Hendron, and Steve Pufka. The authors are grateful to Rohm and Haas for permission to publish this work, and to Bob Opila for accepting the paper for AIChE.

References

1. S. Sundararajan, D. G. Thakurta, D. W. Schwendeman, S. P. Murarka, and W. N. Gill, *J. Electrochem. Soc.*, **146** (2) 761 (1999).
2. R. S. Subramanian, L. Zhang, and S. V. Babu, *J. Electrochem. Soc.*, **146** (11), 4263 (1999).
3. D. G. Thakurta, C. L. Borst, D. W. Schwendeman, R. J. Gutmann, and W. N. Gill, *J. Electrochem. Soc.*, **148** (4) G207 (2001).
4. N. Patir and H. S. Cheng, *Trans. ASME*, **100**, 12 (1978).
5. G. P. Muldowney and D. P. Tselepidakis, *Proceedings of CMP-MIC* (2004).
6. G. P. Muldowney, *Proceedings of AIChE Annual Meeting* (2003).
7. G. P. Muldowney, *Proceedings of MRS Spring Meeting* (2004).
8. G. P. Muldowney and D. P. Tselepidakis, *Proceedings of ECS Spring Meeting* (2004).
9. G. P. Muldowney, *Proceedings of CAMP 9th International Symposium on CMP* (2004).
10. G. P. Muldowney, *Proceedings of ECS Spring Meeting* (2004).
11. L. Cook, in *Semiconductors and Semimetals*, **63**, Academic Press (2000).
12. G. P. Muldowney and D. B. James, *Proceedings of MRS Spring Meeting* (2004).
13. S. Ergun, *Chem. Engr. Prog.*, **48**, 89 (1952).

Mirra® is a registered trademark and Orbot^{TM} is a trademark of Applied Materials, Inc. Wyko RollScope® is a registered trademark of Veeco Metrology Group.